CHAPTER 2

LITERATURE REVIEW

2.1 Overview of dragline

The dragline is a heavy-duty, cyclic equipment that moves broken rock material from one position to another while sitting at one position. The conventional role of dragline in an open cut strip coal mine is to uncover the mineral by removing the overburden rocks (Figure 2.1). The dragline mining is a relatively simple, versatile, low- cost, mining method. A single dragline has the capability of operating over a wide range of overburden depths for the different material characteristic (Humphrey,1990).

The first dragline was invented by John W. Page in 1904, the founding father of Page Company. The employer then merged with The Harnischfeger Corporation P and H, in 1988. Other two companies in dragline marketplace, Marion Steam Shovel Dredge and Bucyrus additionally merged under the name of Bucyrus. Today, Bucyrus and P and H are most popular dragline producer in the international market.

Figure 2. 1: Dragline in a coal mine (Anonymous, 2008)

Using the dragline in the mining industry for the removal of the overburden in stripping enhances productivity by up to 40 per cent in comparison to the shovel-truck method (ozdogan,1984). Figure 2.2 shows that the relative changes of unit cost for different stripping ratios, economical advantage of dragline over shovel-truck system (Hartman, 2002).

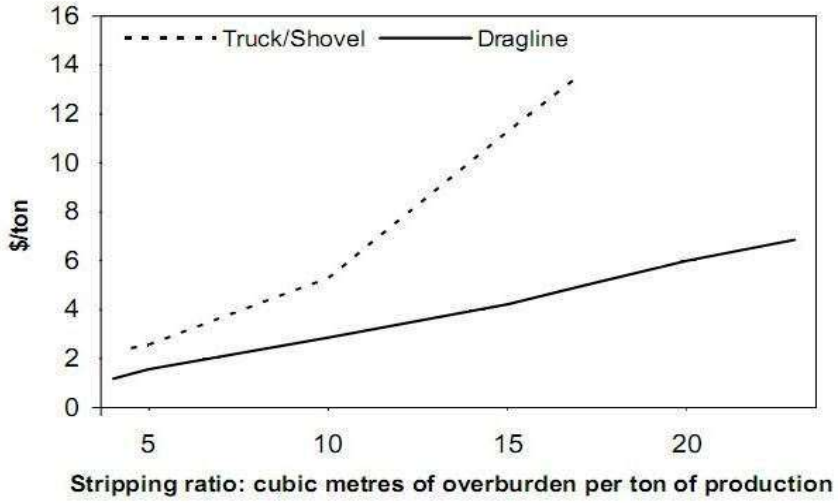

Figure 2. 2: Economic comparison of a truck shovel and dragline (Hartman, 2002)

Different size and capacity dragline are used for different mining applications. There are many factors affecting the method of working with dragline, namely, geology, dragline characteristics, mine production targets, coal and overburden thickness, nature of formation, formation stability of the area, number of coal seams, design of blasting, loose material strength and dragline line operator skills etc.(Mirabeding and Baafi,1998).

Length of a dragline pit is tormented by the factors which include topographical and geological adjustments and human-based handicaps (Hartman,1992). On the other hand, the width of the pit is consistent with, dragline specification inclusive of maneuverability, dumping radius, movement charge, and layout parameters (Hartman,1992).

2.2 Productivity factors of the dragline

As in maximum earthmoving activities, two targets must be managed additionally for an efficient dragline operation, (i) minimizing the cycle time and maximizing the wide variety of cycles and (ii) maximizing the payload of the bucket (Vynne, 2008). Therefore, the detection of influential parameters and the associated statistics in both cycle time and payload are important to investigate the productivity of dragline operations. Demirel (2009) places these productivity factors into two groups, namely mine-planning and operational factors. Mine makes plans and schedules elements to cover the aspects of dragline operation geometry, the suitability of the dragline for voted production, cost-effective, rehandle excavation volume, blast design satisfying the looseness of the formation, layering of coal, and bucket choice etc. On the other hand, operating factors manage the concerns including the availability of dragline for the operations, running conditions, suspended load, fatigue behaviour due to of loading additives on a dragline, cycle time, operator skill, and preservation software. In this light, Rai's (2000) primary cyclic excavator system, as stated in Equation (2.1), gives a simple technique which is about the positive and negative effecting factors for month-to-month production of a dragline (cited in Demirel, 2007).

$$O = \frac{B \times BF \times HS \times A \times J \times 3600}{(1+S) \times C \times (1+R)} \qquad 2.1$$

Where,

O = Monthly Production (m^3)

B = Bucket Size (m^3)

BF = Bucket Fill Factor (%)

HS = Scheduled Hours per Month (hrs)

A = Maintenance Availability (% of the scheduled time machine is available for stripping/100)

R = Rehandle Ratio (%)

J = Job Factor (% of the time that machine is available for stripping)

C = Average Cycle Time (sec)

S = Swell Percentage / 100

In Equation (2.1), the cycle time of dragline is a vital parameter that is inversely proportional to the dragline productivity. Maximizing the number of cycles and minimizing cycle time may be managed with reducing operational and mechanical delays including idle, swing and return rates, taking walks and fill times, and see time (Vynne, 2008). It is also clear that the performance is linked to the position of the bucket inside the operation; bucket size and bucket fill factors. These parameters determine the payload cast using the dragline. The amount of payload is affected by the factors such as, blasting and looseness of the formation, resistance exhibited against the bucket, accuracy of the weight monitoring system, geology, bucket rigging, specifications of the bucket, suspended load, operator factor (Vynne, 2008). Therefore, formation specifications of the mine site and interaction of bucket with the formation are important to realize loading efficiency of the bucket. Studies about the bucket-formation interaction and bucket productivity can provide advantage to (i) increase the bucket payload, (ii) decrease the cycle time, (iii) prevent unexpected failures and fractures on the bucket components, and (iv) reduce the maintenance cost. Productivity is related to the bucket filling mechanism and load in the dragline bucket. The relation between payload, dig time and productivity are very important. The priority lies in improving by increasing the payload and decreasing the digging and filling time (Ozdogan,2015).

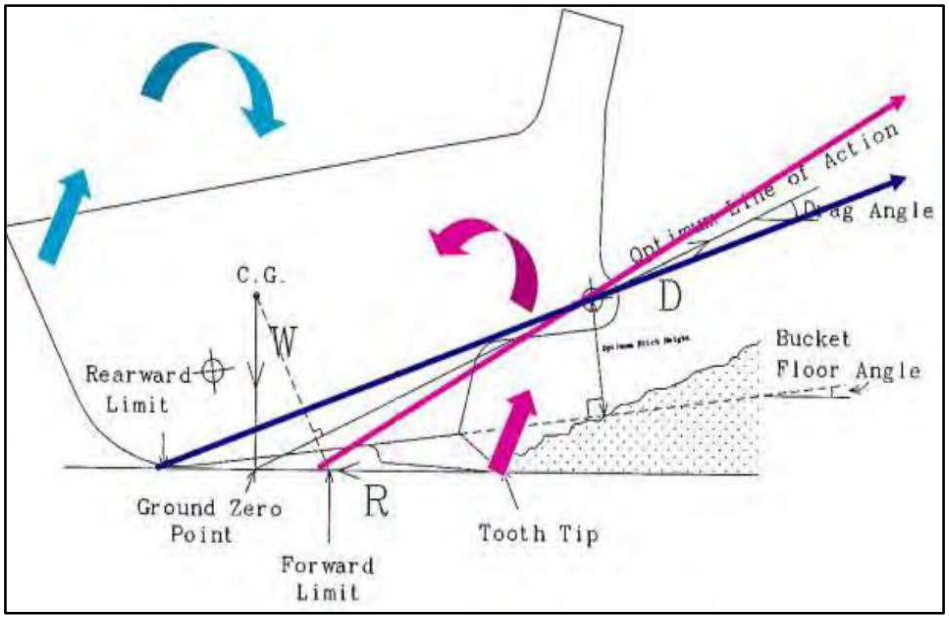

Figure 2. 3: Center of gravity of an arch type dragline bucket (Dragline Dictionary, 2014)

2.3 Dragline productivity studies

For the dragline productivity the common search topic is about the front-end parts of dragline during excavation and their effects over the productivity. A dragline is an earthmover which is operated with its long and heavy boom in a range of curvilinear area. Different amounts of forces and inertia are borne by the distinct parts of the machine at some point of digging, hoisting, revolving and dumping cycles. Ideally, dragline should be controlled in such a manner that maximum amount of payload may be carried at minimal cycle time without catastrophic failure or damages to the operations and operating system. Since these kinds of failures and damages can bring forth long-term breakdowns that badly affects the production and productivity. The research and simulation of the loaded elements of dragline are important to analyze their effects over the dragline performance. Several concepts and theories analysis for of distinct components of dragline have

been practiced in recent years. These researches mainly focus on the topics related to boom structure, rigging mechanism, bucket, and its associated assemblies etc.

In a study of dragline booms, Dayawansa et al. (2006) described stress and failures in the weld joints of the booms. A solid model of the boom was created, which was made of structural tubular elements. Three-dimensional stress analysis of the boom components was done. Effective forces on the boom were detected, which appeared due to the self-weight of the boom, the weight of the bucket acting through the, suspension ropes, hoist ropes and the inertia of angular accelerations. In the study, crack propagation in the boom was examined. In another research, Demirel (2007) modelled the front-end assembly of dragline with kinematic and dynamic variables to find maximum loads over the parts and yield stress of the boom. Figure 2.4 illustrates the two-dimensional view presentation of the front-end assembly, used in the analysis of stress values during dragging and hoisting of the bucket and rotation of the boom. Simultaneous Constraints Method and Discrete Element Method (DEM) were used to formulate the kinematics of dragline and bucket-material interactions, respectively.

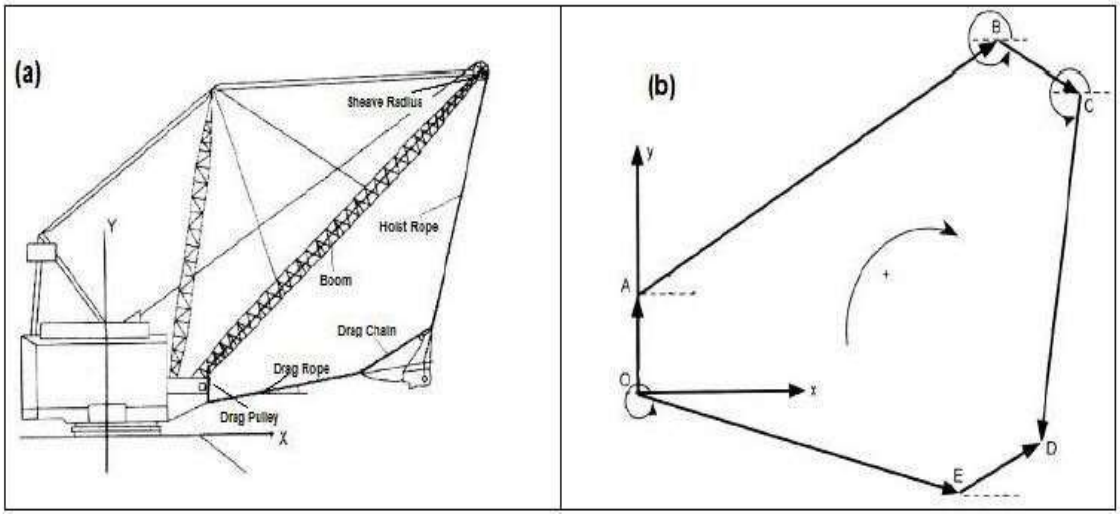

Figure 2. 4: Dragline kinematics (a) Dragline Front-End Assembly (b) Vector Loop Presentation (Modified after Demirel, 2007)

In addition to dragline boom, researches about dragline bucket and rigging machine are equally critical, because of the fact that dragline bucket is interacting with the ground. Draglines make overburdening operation with their massive earth digging buckets, some of which can remove earth greater than 108 m^3 (140 yd^3) right away (Gilewicz, 1999).

The bucket of dragline is mounted to the truss-structured boom with supporting cord ropes. Movement and manoeuvre of the bucket are carried out by several chains and ropes, called rigging mechanism (Figure 2.5). The rigging mechanism specifically ballasts the bucket. Furthermore, cord ropes help the vertical and horizontal moves of the bucket. There are two types of ropes, drag rope, and hoist rope which are powered using electric or diesel type motors. While the hoist rope helps the suspending bucket to move upward and downward, the drag rope pulls the bucket horizontally. In a dragline operation, all external stresses acting on the dragline, rise from the interaction between formation and bucket. Therefore, design and simulation of the bucket and its related assembly are important for the general performance of the dragline.

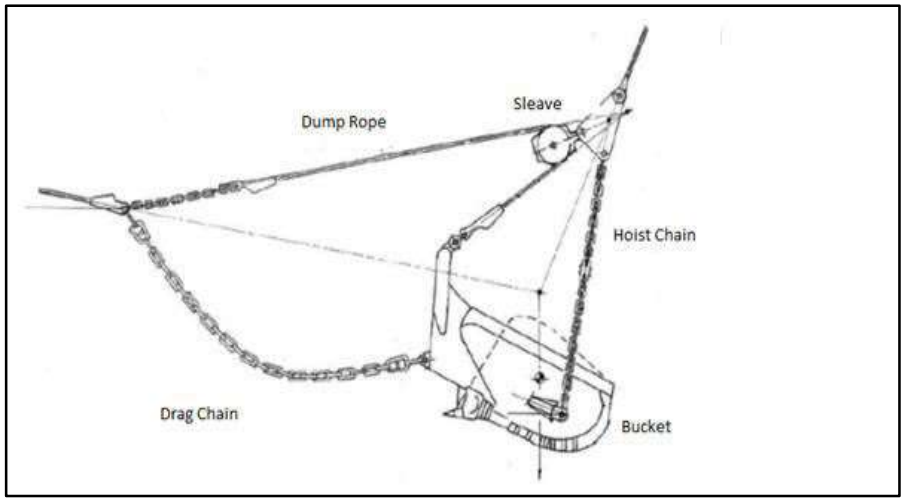

Figure 2. 5: Dragline bucket and rigging mechanism (Modified after Ridley, 2004)

Design of a dragline bucket includes the dimensional and weight parameters depending on the selection of lip type, shape of the tooth and its number, bucket rigging mechanism, and it affects the overall productivity of dragline operation (Ozdogan,2003) Therefore, many research studies have been carried out to improve the bucket and rigging system of dragline. Ridley and Algra (2004) classified the investigations about the productivity studies for bucket and rigging mechanism into four main groups: Optimization of bucket filling, improvement of the rigging system, testing of bucket kinematically, and automation of scooping.

2.4 Design and filling of excavator bucket

The filling of an excavator bucket is a complex granular flow problem. Using the discrete element method (DEM) approach to model soil-implement inter-action, the filling process of an excavator bucket was simulated (Coetzee, Els,2009). While filling of buckets in the absence of very large rocks, it has been observed that the process can be simulated as the two-dimensional case with little motion in the transverse direction. The flow pattern along a cross-section of the bucket in the drag direction is the most important aspect of filling and has been analyzed satisfactorily using 2-D model analysis (Cleary,1998).

An excavator analysis consisting of an articulated arm (backhoe), bucket and cab mounted on a pivot at a top and undercarriage with tracks or wheels has been cited in the literature. The study of the component of the excavator to identify the problem faced while performing the lifting and digging operations by such excavators have been done. Such excavators filling process has been modelled as a 3D solid model of the excavator arm linkage with the help of Pro-e software and analysis was done in Ansys software (Bende, Awate,2013). Tupkar and Zaveri (2015) evaluated the excavators used in construction operation, for example,

digging, levelling of ground, carrying materials, dumping materials and other operations. They thoroughly assessed the possibility of failure or breakage of teeth and evaluated the stresses developed at the tip of excavator bucket teeth. The bucket wheel shaft is one of the highest loaded components in bucket wheel excavator. The bucket wheel excavator failure occurred in a brown coal mine due to the fractured shaft of the bucket wheel. Hence, a discrete model of the shaft was built, and numerical simulation of the shaft operation using the FEM method was done. Macroscopic and microscopic images of the fractured area were obtained and prognosticated for the future (Rusinski et al.,2010).

About the bucket filling, O'Beirne (1997) tried to locate the consequences of adjustments on the rigging mechanism in the bucket performance. Within the scope of the research, differences among rigging device utilization in Australian mines, influences of rigging components such as hoist rope, unloading rope, chain on the bucket efficiency were analysed. Kavetsky (1999) developed a computational tool for application during the design and optimization of bucket and rigging device. Some computational modules were created to prepare a CAD environment for bucket design in order to create two-dimensional bucket and rigging mechanism models, to determine material particle specifications, and to validate and display the program results. In another dragline bucket productivity investigation, Townson (2001) researched the optimization bucket payload of the dragline. For this, special mechanical and finite detail models were created, and it was successfully demonstrated with website test measurements for a Bucyrus type dragline. In the study, it was aimed to analyze the relationship between bucket filling and idle time, which occurs due to the high wearing. As an example, to the simulations about dragline bucket, Coetzee et al. (2007) used the DEM and

Material-Point Method (MPM) to analyze the weight in the bucket of the excavator. During the digging period, go with the flow of the material over the bucket of an excavator and most stresses on the tooth have been mentioned, as visualized in Figure 2.6. In another work about buckets, Cleary (1998) searched and compared, the filling performances of two special designs of dragline bucket with the assist of DEM. Besides the investigation about material swelling during the filling, erosion effects of the particles on the wearing were also tried to be inferred from the kinetic energy changes and particle collision angle.

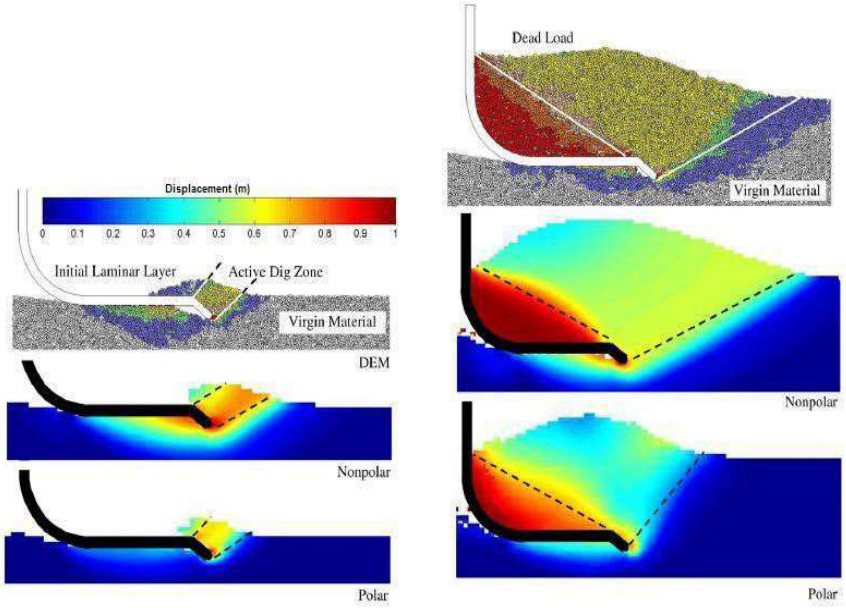

Figure 2. 6: Shear zone theory at different displacements (Coetzee, 2007)

For improvement of the rigging system and its performance, Rowlands (2000) reported on universal rigging system, which is different from the conventional rigging with its distinct hoisting rope configuration. A dragline prototype with a 1:250 scale was examined for this purpose. After tests, it was observed that universal rigging system provides benefits with a decrease in capital cost of rigging components, duration of idle time, cost of installation, and an increase in possible dumping height and chopping reach. It was also claimed that this system

was capable of limiting the transient forces on the dragline with its semi-automatic control. Meyers and Leslie (2001) worked on the effects of the pivot point differences of a common rigging mechanism, front hoist, drag, and rear hoist points, on the performance of bucket. In the study, total mass reduction and new mass distribution of each bucket and load variations, payload according to new configurations of ropes had been discussed, and performances of conventional rigging mechanism and universal rigging mechanism were as compared.

In respect of the kinematics of the dragline bucket, Srour (1999) claimed to have created a simulation model identifying bucket and its rigging system with the help of a data set. It was expressed that this model could solve non-linear equations for the static equilibrium of the bucket and rigging. It was also stated that the model could assess the static force distribution and carrying angle of the system when any change of the bucket and rigging mechanism was introduced in the model. Furthermore, Ridley et al. (2004) tried to explain the bucket and rigging dynamics of dragline with a numerical model and simplified laboratory experiments. In the look at, a dynamic model has defined the perturbation of the bucket from a static equilibrium point of view. The static posture of the dragline bucket and rigging with a contour set of equal buckets carry angle was defined as in Figure 2.7. Initial angular accelerations had been decided with the help of hoist and drag rope tensions and the static load. After the computation procedure, solutions of the numerical model were compared with the experimental results.

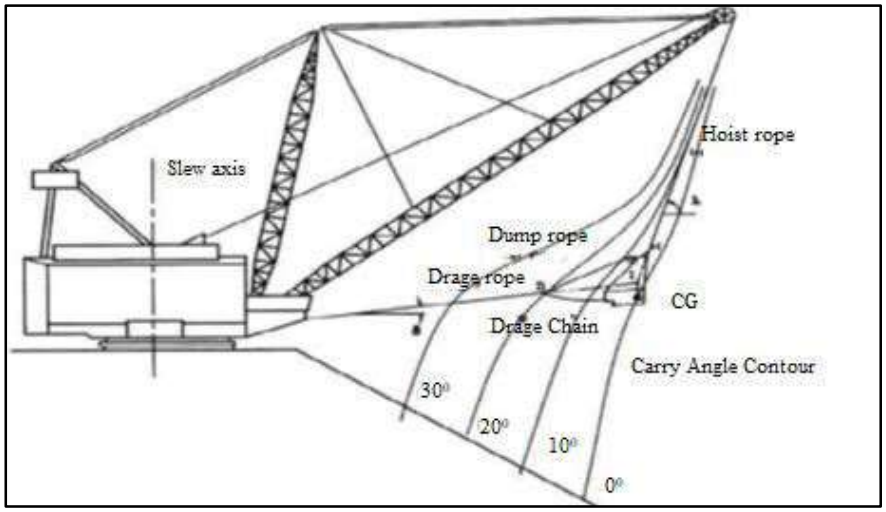

Figure 2. 7: Dragline layout showing constant carry angle contours (Ridley, 2004)

About the automation of dragline, Lever and McAree (2003) aimed to draw a roadmap for determining the requirements of the scooping automation in open-cast mines. In this perspective, areas were identified and surveyed to enhance productivity and to reduce the number of failures with the help of advanced sensor-based technology, existing sensor systems mine-wide information system, on the sites.

In addition to the researches in, bucket and rigging gadgets, investigations of bucket tooth are of vital significance. Since dragline buckets use teeth mounted at the front lip to penetrate and cut the formation for earthmoving activity. A typical tooth is either single-part with wedge shape or two-parts consisting of tooth holder and tooth point (Figure 2.8). For two-part teeth, there is a nose part in the front of bucket lip to weld the removable teeth holders on it and to mount the replaceable teeth factors to the holders. Ryerson (1980) indicated the assembly of these two parts extends about 66 cm from the lip part in 46 m^3 (60 yd^3) buckets where it extends forward about 76 cm from the lip part in 92 m^3 (120 yd^3) buckets. Moreover, Ryerson (1980) expressed that a 25cm width bucket tooth point can weigh up to 68 kg, tooth holder 177 kg and tooth base 385 kg to overcome the

high level of formation stress during the digging and to resist the breakages on the tooth assembly. In the present research work, a single-part tooth with a wedge shape is used.

Figure 2. 8: Dragline bucket teeth (a) Single Part (b) Double Part

2.5 Force impacting the stability of equipment

In dragline, there are many phases of digging comprising of penetration and break out steps of the bucket. During penetration of teeth on the blasted bench, the bucket is dragged towards to the machine via drag rope and rock material is broken out and the bucket is filled. During this mechanism or process forces affecting dragline bucket, breakout force and bucket fill mechanism have been investigated. Penetration capability of buckets manufactured by well-known manufactures is higher. On such buckets, the whole weight of the bucket is transferred on the teeth with an optimum cutting angle (Ozdogan,2015). The optimum carry angle β should be $25^0 \geq \beta \geq 15^0$, which can be adjusted by the length of drag and hoist chains (Ozdogan,2015). The following equation has further been suggested to determine the optimum bucket fill distance in the blasted muck.

B.F.D., m= (1.5 to 3) ×B. L

Where,

BFD = Bucket fill distance, m.

BL= Bucket length, m.

2.5.1 Break out force and penetration effect

Break out force is the drag-force applied to the bucket by the drag rope. This force has to overcome the dead weight of the bucket; the overburden material fills in the bucket. The friction force acts between the bench surface and the base of the bucket and the resistance of the rock mass to digging are illustrated in Figure 2.9 (Ozdogan,2015).

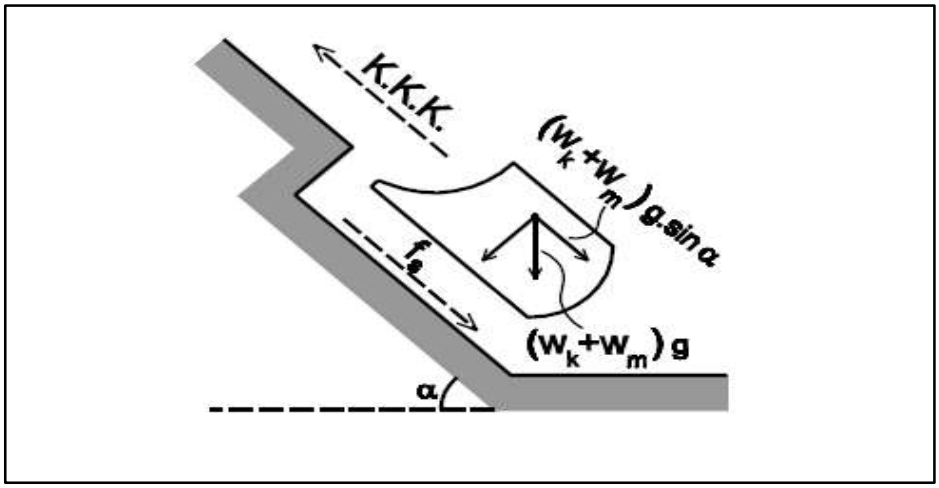

Figure 2. 9: Forces affecting the bucket during normal bench digging (Ozdogan,2015).

The importance of knowing payload in the bucket is invaluable information and indicates as to how the dragline bucket performs. A case study has been reported on a 31m^3 capacity bucket of walking dragline for determining the energy consumption per ton of rock in the bucket (Ozdogan, Ozgenoglu,2009).

Bucket penetration mechanism of walking dragline at the digging bench has been investigated. The tare weight of the bucket assists in the penetration. There are some important factors affecting the bucket penetration like bucket penetration angle, bucket weight, bucket teeth and excavation bench slope angle (Ozdogan,2015).

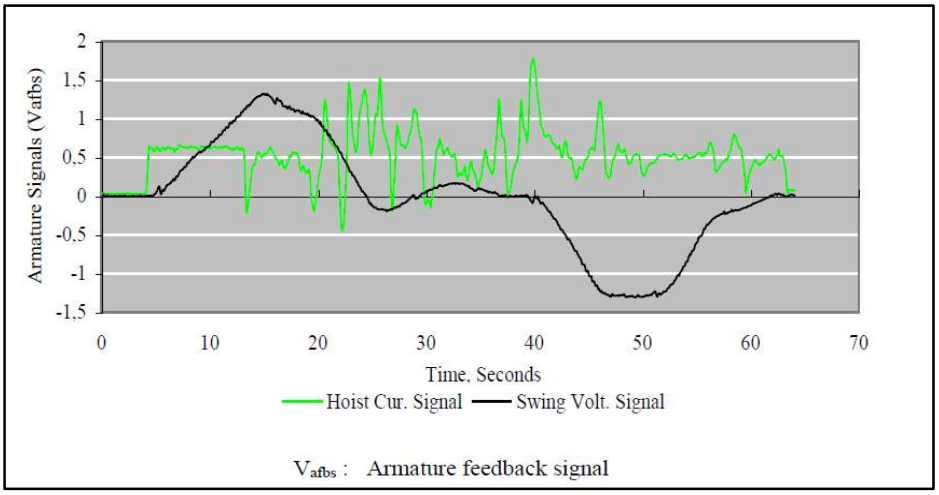

Figure 2. 10: Time vs hoist current - swing voltage signals of empty bucket digging cycle, Ozdogan (2002).

Bucket penetration in bench rock whether it is blasted or not is governed by the weight of the bucket. The force generated by the empty bucket is exerted to the bench material via bucket teeth and its penetration (Ozdogan,2015).

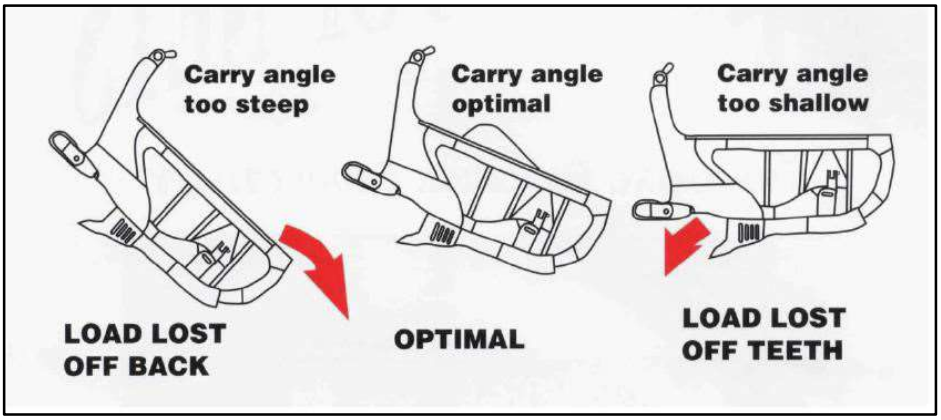

Figure 2. 11: The perfect carry angle of a dragline bucket (Beatty,1996)

As seen in Figure 2.11 bucket having good design and manufacture have optimum penetration, fast filling time and have optimum carry angle so that there is a minimum load lost. Generally, an acceptable carry angle varies between 15^0 to 25^0 (Beatty,1996).

2.6 Finite element analysis

The finite element method usually abbreviated as FEM is a numerical technique to obtain an approximate solution to physical problems. FEM was initially developed to study stresses in complex structures. It has since been extended and applied to the broad field of continuum mechanics, including fluid mechanics and heat transfer. Because of its capability to handle complex problems and its flexibility as an analysis tool, FEM has gained a prominent role in engineering analysis and design.

The finite element method is a very versatile numerical technique and is a general-purpose tool to solve any physical problems. It can be used to solve both field problems and non-field problems. The most important advantage is that FEM is well suited for a problem with complex geometries because no special difficulties are encountered when the physical domain has a complex geometry. The other significant advantage is that it is easier to write general-purpose computer codes for FEM formulations.

2.6.1 Finite element formulation

The main drawback of the weighted residual method is that it is difficult to find good trial functions because one may not have any prior knowledge of the behaviour of the solution y(x). Polynomials are often selected as trial function in such cases and might do a poor job of interpolation (we can think of f(x) as an interpolation function between the boundary conditions that also satisfies the differential equation), especially when the interval [a, b] is large.

Through experience, it is known that low-degree polynomial can reflect the behaviour of the function if the interval [a, b] is short. So, we hope to successfully apply the weighted residual methods using low-degree polynomials by

subdividing the interval [a, b] into smaller subintervals. That is, we use piece-wise lower degree polynomials in smaller subintervals rather than going for a higher degree polynomial for the entire domain. This is the strategy used in the finite element method (Salih, 2018).

2.6.2 Steps in FEM

The major steps involved in the solution of a problem using FEM are:

- The solution interval (domain) is discretized (subdivided) into several small non-over- lapping subintervals (subregions) referred to as finite elements. These elements join at x1, x2, ⋯, xn−1. Add to this array x0 = a and xn = b. We call the xi's nodes of the elements.

  The process of discretization is essentially an exercise of engineering judgment. The shape, size, and number of elements have to be chosen carefully in such a way that the original domain is simulated as closely as possible without increasing the computational efforts.
- Select an approximating function known as interpolation polynomial for f (x) to represent

  the variation of the dependent variable y(x) over the elements.
- Apply the Galerkin method to each element separately to interpolate (subject to the differential equation) between the end nodal values, f (xi) and f (xi), where these f (xi)'s are approximations to the y(xi)'s that are the true solution to the differential equation.
- The result of applying the Galerkin method to element (e) is a pair of equations in which the unknowns are the nodal values at the ends of element (e), the c's. When we have done this for each element, we have equations that involve all the nodal values. Assembly of the element equation to form the global equation for

the problem. It produces a system of algebraic equations and one equation for each element.

- These equations are adjusted for the boundary conditions and solved to get approximations to y(x) at the nodes, and we get intermediate values for y(x) by linear interpolation.
- The system of algebraic equations are then solved to get the approximate solution f (x) of the problem.

2.6.3 Selection of elements

One of the most important steps in finite element analysis is the selection of the finite elements and the definition of appropriate approximating function within the element. The approximating function is referred to as interpolation polynomial. Each element is characterized by several features. So, when somebody asks 'what type of element you are using' for a problem, he is asking for four distinct pieces of information (Salih, 2018).

- The geometric shape of the element, is a line segment, triangle, rectangle, tetrahedron, etc.

- The number and types of nodes in each element, whether the element contains two nodes or three nodes etc. By type of nodes, we mean whether the nodes are interior or exterior. Exterior nodes are the nodes that lie on the boundaries of the element, and they represent the point of connection between bordering elements. Interior nodes are the nodes that do not connect to the neighbouring elements.

- The type of the nodal variable. Depending upon the problem, the nodal variable may have a single degree of freedom or several degrees of freedom.

- The type of the approximating function is polynomial, trigonometric functions etc. Polynomial approximating functions have found widespread acceptance because they are easy to manipulate mathematically (Salih, 2018).

In this thesis, the shape of the element is taken tetrahedron for the analysis purpose. If anyone these characteristic features are missing, the description of the element is incomplete.

2.6.4 Properties of the shape function

- Several shape functions of an element depend on the number of nodes in the element. Each shape function is associated with a unique node.
- Each shape function has a value of one at its node and zeroes at the other nodes.
- The sum of the shape function is equal to one everywhere within the element.
- The shape functions and the interpolation polynomial of an element are of the same types. If the interpolation polynomial is quadratic, the resulting shape functions are also quadratic.
- The derivative of the shape functions concerning the independent variable sums to zero.

These properties are valid for all types of element, whether it is one-dimensional, two- dimensional, or three-dimensional element with polynomial as interpolation polynomial (Salih, 2018).

2.6.5 Applications of FEA

- Mechanical/Aerospace/Civil/Automotive Engineering
- Structural/Stress Analysis
    - Static/Dynamic
    - Linear/Nonlinear

- Fluid Flow
- Heat Transfer
- Electromagnetic Fields
- Soil Mechanics
- Acoustics
- Biomechanics

2.7 Finite Element Analysis for Earthmoving

2.7.1 Basic idea of finite element analysis

Finite element analysis (FEA) has been used for analysis and simulation under different loading conditions of the excavator components. The FEM analysis of any structural element supports in forecasting the structural masses and design in which it will act under stressed conditions (Azam and Rai,2018). Finite Element Analysis (FEA) is a computational simulation approach imparting one-of-a-kind possibilities to analyse physical conditions such as displacement, stress and strain, force, velocity, acceleration, mass on stable bodies by the use of a numerical identity known as a finite element. FEA drives complicated configurations of factors named as a node. It generates adjacent grids named as mesh, the usage of the nodes. The mesh has a network formation where each adjacent node is connected. This mesh network involves material and structural specifications to identify how the structure will respond to different analysis conditions. As an example, to FEA utility, a blade cutting operation is illustrated in Figure 2.12. Structural analysis in FEA carries linear and nonlinear models. Linear functions make use of simple parameters and assume that the deformation of a material isn't plastic. On the alternative hand, nonlinear functions can examine the stress on the

fabric while the elastic functionality of it is surpassed. Therefore, stress values in nonlinear functions keep changing with plastic deformation.

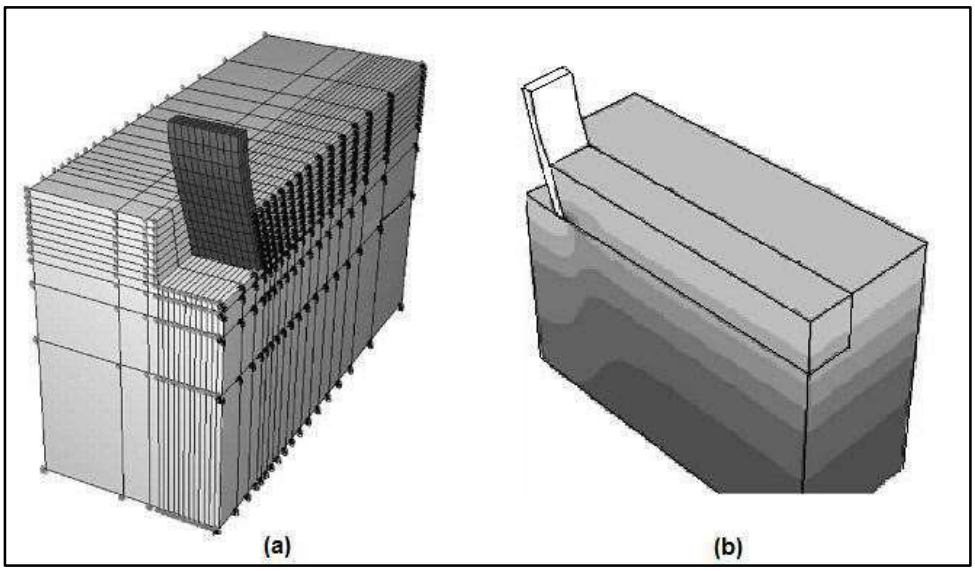

Figure 2. 12: FEA (a) Meshing (b) Stress Distribution (Abo-Elnor et al. 2004)

2.7.2 Applications of finite element analysis in earthmoving equipment

An earthmoving action expresses the shape of interaction between the formation and the digging tool. This interaction is mainly affected by formation specifications such as density, internal friction angle, external friction angle, cohesion and adhesion.

Earthmoving elements shape an entirely complicated phenomenon. The formation can exhibit either isotropic or anisotropic nature. If it is anisotropic, formation specifications change mainly with the direction of forces inside the formation, and it is hard to estimate such behaviour. Moreover, compactness of the formation can entirely change the influence on the digging tool. All dynamics of the formation are required to be known to see the full interaction between tool and formation. However, it is hard to identify the full effect of the formation on the tool. Under these conditions, it is better to characterize the tool-formation interaction in reality, with some assumptions.

Many investigators have used FEA to address troubles related to earthmoving movements. Yong and Hanna (1977) worked on the productivity of a flat blade moving in clay formation for a distance smaller than one foot. It was claimed that they proposed a method that gave a unique value of the stress and deformation of the formation due to the excavation forces. It was stated that the method provided advantage in the estimation of forces exerted by both the tool and the formation.

Mounem and Nemenyi (1999) created an elastic-perfectly plastic formation model and used FEA to simulate the formation cutting process of a sub formation for varying geometries. Fielke (1999) performed a computational model expressing the effect of cutting-edge geometry over the tillage forces. The experimental results supported this two-dimensional finite element model. Mootaz et al. (2003) performed the three-dimensional simulation of narrow blade-formation interaction in an FEA solver, by assuming that formation behaves elastically. They tested formation failure zones vertically and horizontally to eliminate convergence trouble precipitated due to large blade movement. The model was validated by providing the ultimate shear stress zones in the formation after computing the software and matching it with the predefined formation failure areas. In a two-dimensional approach, Davoudi et al. (2008) insisted that a model which is capable of estimating draft forces during tillage was created in FEA software. Moreover, in many research, brittle behaviour and plasticity of formation during the cutting process was analyzed (Chi and Kushwaha, 1989; Raper and Erbach, 1990; Aluko and Chandler, 2004; Aluko, 2008).

Besides FEA, the reader can decide on to use DEM for the tool-formation interaction modelling, although it is mainly deployed for the simulation of

granular materials and for analysing the connection among inter-particle and particle-tool behaviours (Cleary, 1998; Owen et al., 2002; Hofstetter, 2002).

2.8 Tool-formation of dragline bucket in earthmoving conditions

An earthmover performs two important earth digging mechanisms inclusive of cutting and penetration, consistent with their digging device geometries and formation displacement abilities. When the shape of the digging tool is handled, the bucket includes explicitly two elements, as shown in Figure 2.13. Initially, the bucket has a square shape ground component, named as the separation plate marked as A in Figure 2.13. With the help of this plate, a bucket can transverse the formation by pushing and dragging (dragline bucket) it in the blasted material. Secondly, the bucket has another important ground interacting component, viz teeth, marked as B in Figure 2.13. Bucket teeth penetrate the formation media to relieve the digging mechanism.

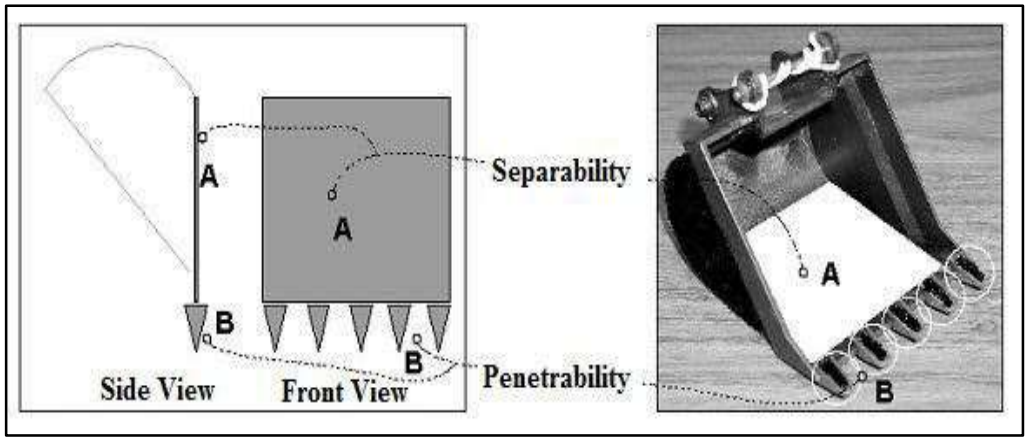

Figure 2. 13: Penetration and separation parts of a bucket

Figure 2.14 illustrates the varieties of earthmoving actions for a dragline bucket. As seen in Figure 2.14, the bucket firstly penetrates the formation with the help of its weight and then, cut it along the operation direction. Figure 2.15 indicates the orientation of a dragline bucket with the formation at some stage in operation.

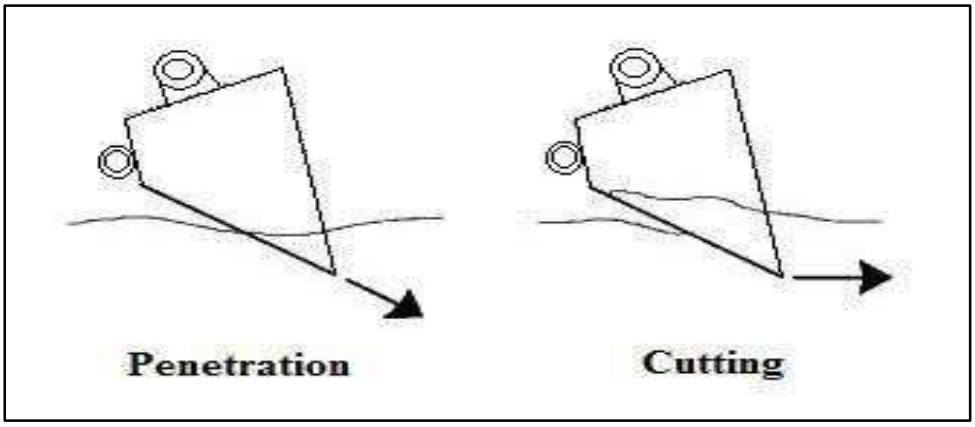

Figure 2. 14: Fundamental earthmoving actions for a shovel (Modified after Blouin, 2001)

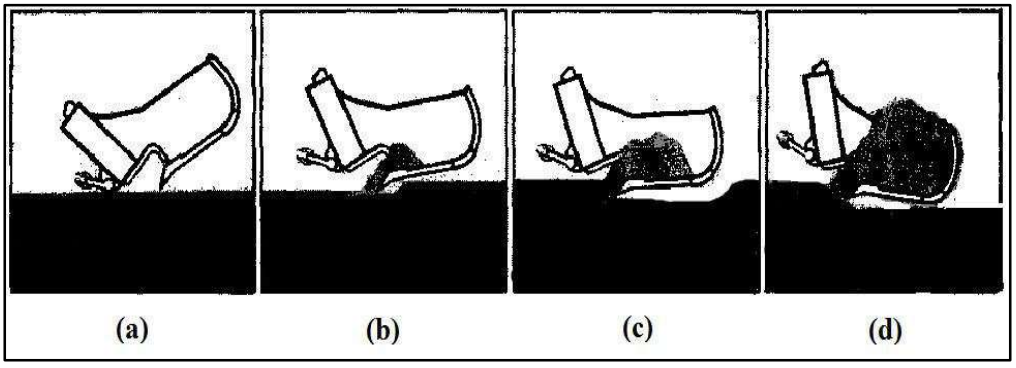

Figure 2. 15: Dragline bucket earthmoving actions (Ozdogan, 2003)

2.8.1 Cutting resistance model for empirical approaches

The question about the resistance of formation during the machine cutting operation has been one of the primary interests in surface mining and construction machinery, aerospace earthmoving, and agricultural tillage fields. At this point, empirical approaches can help to find beneficial information about this question. Some researchers have tried to calculate cutting resistance of the formation based on empirical outcomes for distinct earthmoving machines (Alekseeva et al., 1985; Zelenin et al., 1986; Nedoredzov, 1992, and Hemami et al., 1994).

A few empirical approaches for estimating a cutting tool-formation force were made by Zelenin et al. (1986). In one of the studies, the cutting resistance model was formed for a bucket without teeth. The model considers the factors such as

the condition of formation, cutting conditions and geometry of the digging tool, as shown in Equation (2.2).

$$P = 10C_o e^{1.35}(+2.6b)(+0.0075\alpha_c)(+\ 0.03s)\alpha_0\, k \qquad (2.2)$$

In Equation (2.2), P is cutting resistance, C_0 is compactness coefficient, e is cutting depth in cm, b is bucket width in m, α_c is the angle of cutting in degrees, s is bucket cutting surface thickness in cm, α_0 is tip angle coefficient, k is cutting-type coefficient.

2.8.2 Cutting resistance model for analytical approaches

Models used for the force estimation in earth-moving activities aim to find mathematical approaches for the counterforce behaviour of formation on the moving tool. These models can be divided into three most important classes in keeping with the forms of earth-moving activities, penetration, cutting, and loading. Draglines perform the excavation operations with dragging, hoisting, and swing functions. It cuts the formation with its dragging function. Therefore, resistive force models for the cutting action are critical to estimate the stresses over the bucket.

In this perspective, Blouin et al. (2001) presented a review study about the force prediction models for earth-moving tasks. In the review, it was emphasized that three-dimensional cutting models are different from the two-dimensional cutting models due to their side effects. However, Blouin et al. (2001) also stated that there is a negligible relationship between side effect findings of three-dimensional analytical models and those of a real bucket. Blouin et al. (2001) also indicated that it could be utilized from two-dimensional models in force calculation of bucket digging process. Therefore, two-dimensional models will be analyzed and discussed under this title.

i. Model proposed by Osman (1964)

In the two-dimensional models, forces at the surface of the reducing plate are calculated in two-dimensional views (Figure 2.16). For instance, Osman (cited in Blouin et al. 2001) applied from the logarithmic technique to formulate dimensional reducing action. Both the behaviour of heavy medium without surcharge and cohesion and the behaviour of weightless medium with surcharge and cohesion have been protected within the version as equation components. The resultant cutting force is calculated, as given in Equation (2.3).

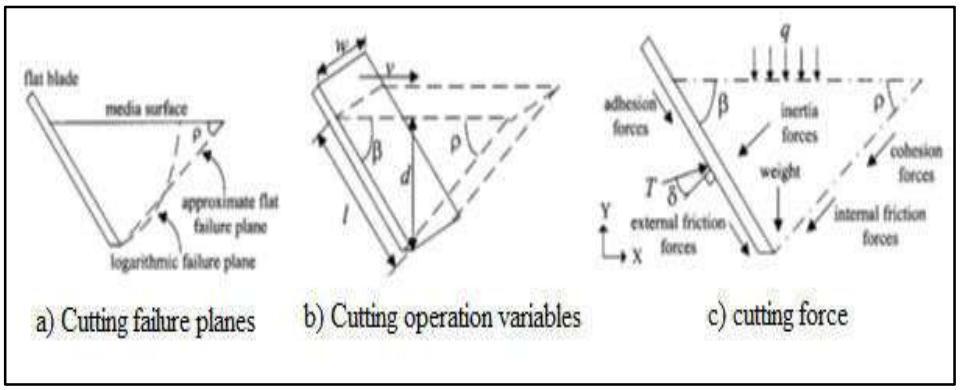

Figure 2. 16: Failure plane in formation cutting (Blouin et al., 2001)

$$T = w[(0.5\gamma t^2\, tan^2\,(45 + 0.5\rho)d_1 + \frac{e^{2wtan\rho}-1}{4tan\rho} r_0^2\ \gamma d_2\ + qttan^2\ (4\ +$$

$$0.5\rho)d_4\,)d_3^{-1}\ + (0.5(r_1^2\ -\ r_0^2)\frac{c}{tan\rho} + 2ctan(45 + 0.5\rho)d_4 +$$

$$\frac{qt}{sin(45-0.5\rho)} d_s + C_a l d_7)d_6^{-1}] \qquad (2.3)$$

In this equation (2.3), T is a resultant cutting force, γ is a specific weight, w is a tool width, d is a tool depth, *l* is a tool length, C_a is an adhesion, c is a cohesion, t is a depth of Rankine Zone, ρ is a shear plane angle, r_o is a curvature radius and d_1……d_7 are graphical distances.

Projection of the resultant cutting force on the horizontal plane is in Equation (2.4).

$$H = Tsin(\beta + \delta) \tag{2.4}$$

In Equation (2.4), H is a horizontal force, β is rake (cutting) angle, and δ is external friction angle. Unlike Osman's formula, Gill and Vanger Berg (cited in Blouin et al. 2001) insert the influence of weight and inertia factors to the cutting force calculation as in Equation (2.5)

$$H = N_o sin\beta + \delta N_o cos\beta + kw \tag{2.5}$$

In Equation (2.5), N_0 is the inertia factor, and the parameter k is related to the wearing factor of the material. It is taken into consideration in case of high wearing. Therefore, re-arranged version of the formula is given in Equations (2.6) and (2.7).

$$H^* = H - kw = N_O sin\beta + \delta N_o cos\beta \tag{2.6}$$

In equation 2.6

$$H^* = [\gamma \frac{sin(\beta + \rho)}{sin\rho}(l + \frac{dcos(\beta + \rho)}{2sin\rho} + \frac{dsin(\beta + \rho)tan\beta}{2sin\rho}) + \frac{c}{sin\rho(sin\rho + \varphi cos\rho)} + \frac{\gamma v^2 sin\beta}{gsin(\beta + \rho)(sin\rho + \varphi cos\rho)}]. \frac{wd(sin\beta + \delta cos\beta)(sin\rho + \varphi cos\rho)}{sin(\rho + \beta)(1 - \varphi\delta) + cos(\rho + \beta)(\varphi - \delta)} \tag{2.7}$$

Equation (2.7), φ is the internal friction angle, v is tool speed, and g is gravitational acceleration.

ii. Model proposed by McKyes's (1985)

McKyes's earthmoving model (cited in Blouin et al. 2001) is the complete form of two-dimensional earthmoving theories which contains factors of weight, cohesion, adhesion, surcharge, and inertia. A simple version of the model is in Equation (2.8).

$$T = w(\gamma g d^2 N_\gamma + cdN_c + C_a dN_{ca} + qdN_q + \gamma v^2 dN_a) \quad (2.8)$$

In equation 2.8 N_γ is a weight coefficient, N_c is a cohesion, N_{ca} is an adhesion coefficient, N_q is a surcharge coefficient, and N_a is an inertia coefficient.

Where

$$N_\gamma = \frac{(cot\rho + cot\beta)\,[sin\theta cot(\beta+\varphi) + cos\theta]}{2cos(\rho+\delta) + sin(\rho+\delta)cot(\beta+\varphi)} \quad (2.9)$$

$$N_c = \frac{1 + cot\beta cot(\beta+\varphi)}{cos(\rho+\delta) + sin(\rho+\delta)cot(\beta+\varphi)} \quad (2.10)$$

$$N_{ca} = \frac{1 - cot\rho cot(\beta+\varphi)}{cos(\rho+\delta) + sin(\rho+\delta)cot(\beta+\varphi)} \quad (2.11)$$

$$N_q = 2N_\gamma \quad (2.12)$$

$$N_a = \frac{tan\beta + cot(\beta+\varphi)}{[cos(\rho+\delta) + sin(\rho+\delta)cot(\beta+\varphi)]} + (1 + tan\beta cot\rho) \quad (2.13)$$

An extended form of McKyes's Model (1985) is visualised in equation (2.14)

$$T = \frac{wd}{cos(\beta+\delta)+sin(\beta+\delta)cot(\rho+\varphi)}\left[\frac{\gamma gd(cot\beta+cot\rho)}{2}+q(cot\beta+cot\rho)\right.$$
$$+\ c(1+cot\rho cos(\rho+\varphi))\ +\ C_a.(1\ -\ cotcot(\rho$$
$$\left.+\varphi))\right.$$
$$\left.+\frac{\gamma v^2(tan\rho\ +\ cot(\rho+\varphi))}{1\ +\ tan\rho cot\beta}\right] \quad (2.14)$$

The horizontal force acting in McKyes's earthmoving model (1985) is in Equation (2.15).

$$H\ =\ Tsin(\beta+\delta) \quad (2.15)$$

iii. Model proposed by Swick and Perumpral's model (1988)

Swick and Perumpral (cited in Blouin et al. 2001) improved Gill and Vanden Berg's model and created an analytical model which covers the effects of adhesion, cohesion, surcharge, weight, and inertia. Swick and Perumpral's model (1988) is shown in Equation (2.16).

$$T = \frac{wd}{sin(\beta+\varphi+\rho+\delta)}\left[\frac{-C_o cos(\beta+\varphi+\rho)}{sin\beta}\ +\ \frac{\gamma d^2}{4}\ (cot\beta\right.$$
$$+\ cot\rho)sin(\varphi+\rho)\ +\frac{qd}{2}\ (cot\beta\ +cot\rho).sin(\varphi+\rho)$$
$$+\frac{ccos\varphi}{sin\rho}$$
$$\left.+\frac{\gamma v^2 sin\beta cos\varphi}{gsin(\beta+\rho)}\right] \quad (2.16)$$

In Equation (2.16), is compactness and cutting index.

Finally, horizontal force in the model is calculated as in Equation (2.17).

$$H = Tsin(\beta+\delta) \quad (2.17)$$

In the thesis study, passive force existed on the bucket due to the interaction with the formation was estimated by McKyes's earthmoving formulation (1985) in Equation (2.8).

The bucket is the primary source of external loads on the machinery since interactions with ground materials take place in this region. So Golbasi and Demirel, 2015 developed a 3 D solid model of a dragline bucket and used the McKyes's equations to evaluate the resistive force in the bucket movement. Use abacus software and simulate the moving bucket using finite element analysis and sensitivity analysis examined the effect of the formation.

2.9 Failure analysis criteria

A range of theoretical standards was proposed each in search of to acquire good enough correlation between envisioned factor existence and that achieved underneath carrier load conditions for both brittle and ductile material packages. The five main theories are:

a. Maximum principal stress theory (Rankine).

b. Maximum shear stress theory (Guest-Tresca).

c. Maximum principal strain (Saint-Venant).

d. Total strain energy per unit volume (Haigh).

e. Distortion energy theory (Von Mises yield criterion).

In this thesis dissertation, energy theory (Von Mises yield criterion) for analysis has been used. According to this theory, yielding would occur when total distortion energy absorbed per unit volume due to applied loads exceeds the distortion energy absorbed per unit volume at the tensile yield point (Hearn,1997). Total strain energy ET and strain energy for volume change EV can be given as:

$$E_T = \frac{1}{2}(\sigma_1\epsilon_1 + \sigma_2\epsilon_2 + \sigma_3\epsilon_3) \quad (2.18)$$

$$E_V = \frac{3}{2}\sigma_{av}\epsilon_{av} \quad (2.19)$$

Substituting strains in terms of stresses the distortion energy can be given as

$$E_d = E_T - E_V = \frac{2(1+v)}{6E}(\sigma_1^2 + \sigma_2^2 + \sigma_3^2 - \sigma_1\sigma_2 - \sigma_2\sigma_3 - \sigma_3\sigma_1) \quad (2.20)$$

At the tensile yield point, $\sigma_1 = \sigma_y$, $\sigma_2 = \sigma_3 = 0$ which gives

$$E_{dy} = \frac{2(1+v)}{6E}\sigma_y^2 \quad (2.21)$$

The failure criterion is thus obtained by equating E_d and E_{dy}, which gives

$$(\sigma_1 - \sigma_2)^2 + (\sigma_2 - \sigma_3)^2 + (\sigma_3 - \sigma_1)^2 = 2\sigma_y^2 \quad (2.22)$$

In a 2-D situation if $\sigma_3 = 0$, then

$$\sigma_1^2 + \sigma_2^2 - \sigma_1\sigma_2 = \sigma_y^2 \quad (2.23)$$

i.e.

$$\left(\frac{\sigma_1}{\sigma_y}\right)^2 + \left(\frac{\sigma_2}{\sigma_y}\right)^2 - \left(\frac{\sigma_1}{\sigma_y}\right)\left(\frac{\sigma_2}{\sigma_y}\right) = 1 \quad (2.24)$$

This is an equation of the ellipse, and the yield surface is shown in Figure 2.17. This theory is accepted to be valid for ductile materials. However, this theory has the following limitations.

- The theory does not apply to brittle materials for which the elastic limit stress in tension and compression is quite different.
- It cannot be applied for materials under hydrostatic pressure.

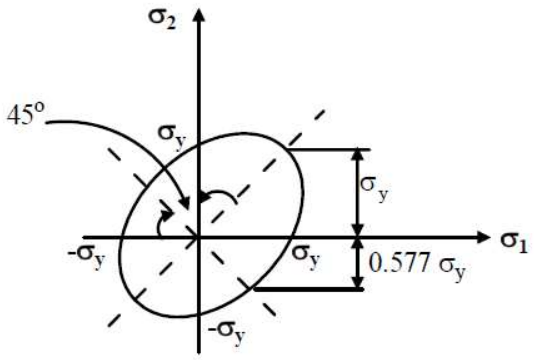

Figure 2. 17: Yield surface corresponding to the Von Mises yield criterion (Hearn,1997).

The value of stress for a particular material used for a specific way, which is considered to be safe stress is usually called the working stress. For static applications, the working stress of ductile materials is usually based on yield strength. The working stress may be considered as either the yield strength or the tensile strength divided by a number called the factor of safety. If failure would result in loss of life, the factor of safety should be increased.

Factor of safety (N) = yield strength/working stress

2.10 Influence of teeth and rake angle on excavator performance

Digging force of electric rope shovel (E.R.S) has two components which are being crowded and bail pull forces. Crowd (penetration) force pushes the dipper into the bank whereas bail pull (breakout) forces move the dipper upward to fil it. The optimisation of hoist and crowd forces are significant in the optimisation of digging depth. Depth of cut is governed by rake and tooth angles of the dipper. Adjustment and optimisation of the rake and tooth angles are absolutely important (Ozdogan, 2016).

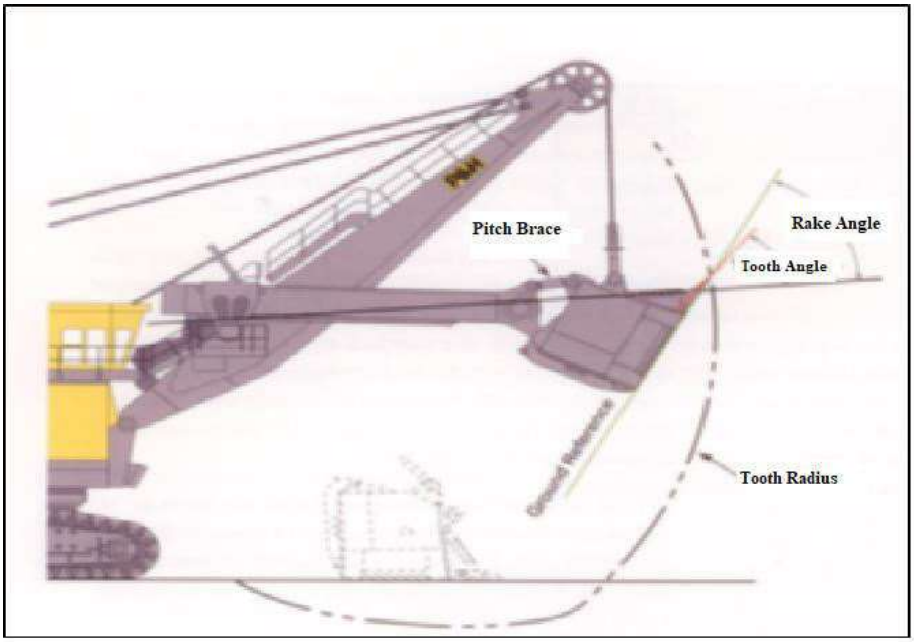

Figure 2. 18: ERS dipper rake and tooth angle, (Anon. a, 2009)

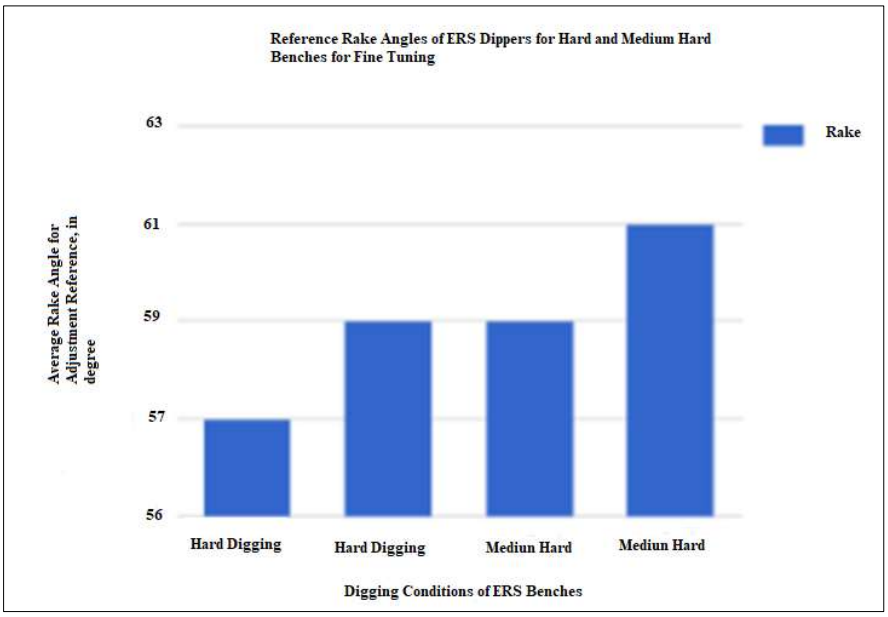

Figure 2. 19: Starting rake angle reference angle ranges to adjust ERS rake angle (Data Anon a, 2009)

The position of the ERS for the best digging performance is where the hoist rope is parallel to the bench face or perpendicular to the ground surface. In this

position, ERS applies the biggest bail pull to the dipper and dipper teeth, and have top digging performance (Ozdogan, 2009).

The analysis was conducted to evaluate the stress distribution on bucket teeth, from the rake angle effect viewpoint, during the excavation. Based on the analysis, the stress distribution and maximum value of stress occurring in the bucket teeth were obtained by varying the rake angles (Suryo et al. 2018).

2.11 Summary of the literature review

Literature survey describes the previous researches in respect of dragline earthmoving operation and theories at the back of this phenomenon. These researches organised a historical past for the thesis challenge, research of stresses on the dragline bucket with FEA. The literature seeks started with the general data about dragline usage on the sector open-cast mines and dragline stripping methods. Then, it proceeded with the investigation of productivity factors which affect the performance of dragline in the field and review of the previous research approximately dragline productiveness.

After a review of dragline and productiveness, literature seeks advanced in a more significant specific subject. In this element, it turned into tried to create a basis for dragline bucket simulation. To attain this, components of finite element evaluation, concepts of earthmoving operations and factors of formation-tool interaction length were analysed.

From the literature survey, it is clearly evident that there exists a gap in the areas of stress investigation and on its operating dragline bucket and its assembly. Therefore, the thesis aims to contribute to the knowledge, with three-dimensional dragline bucket simulation, stress value investigation and effect of rake angle on the tooth of the bucket.